

Electrical, Optical, and Structural Properties of Tin-Doped $\text{In}_2\text{O}_3\text{-}M_2\text{O}_3$ Solid Solutions ($M = \text{Y}, \text{Sc}$)

Andrea Ambrosini, Angel Duarte, and Kenneth R. Poeppelmeier¹

Department of Chemistry, Northwestern University, Evanston, Illinois 60208-3113

Melissa Lane and Carl R. Kannewurf

Department of Electrical Engineering, Northwestern University, Evanston, Illinois 60208-3118

and

Thomas O. Mason

Department of Materials Science and Engineering, Northwestern University, Evanston, Illinois 60208-3105

Received December 28, 1999; in revised form March 23, 2000; accepted April 7, 2000; published online June 27, 2000

In_2O_3 crystallizes in the bixbyite, or C-type rare earth, structure (space group $Ia3$), as do the smaller lanthanide oxides (Tb–Lu) and the oxides of Y and Sc. Solid solutions of $\text{In}_{2-x}M_x\text{O}_{3-\delta}$ ($M = \text{Y}$ or Sc) with varying lattice parameters were prepared and doped with tin. Substitution of tin oxide into $\text{In}_{2-x}Y_x\text{O}_{3-\delta}$ results in the formation of the pyrochlore phase, $\text{Y}_2\text{Sn}_2\text{O}_7$. The pyrochlore dominates the Y–In–Sn oxide ternary phase diagram and prevents the tin from donating charge carriers. Solid solutions in which $M = \text{Sc}$ could be reacted with a limited amount of tin oxide without the formation of a second phase. The presence of increasing scandium results in decreasing conductivity with a corresponding increase in the optical band gap and percent transmission. © 2000 Academic Press

Key Words: transparent conducting oxide; bixbyite; indium oxide; pyrochlore; solid solution; phase diagram.

INTRODUCTION

Transparent conducting oxides (TCOs) are used in a variety of technological applications, including flat panel and liquid crystal displays, solar cells, and electrochromic windows. The TCO currently favored by industry is Sn-doped indium oxide (ITO), which in thin-film form exhibits conductivities on the order of 1000–5000 S/cm and 85–90% transparency across the visible spectrum. ITO, like other related transparent conductors used by industry, is an n -type degenerate semiconductor with an optical bandgap of

about 3.75 eV (1–5). Degenerate semiconductors are highly doped semiconductors in which the localized doping levels coalesce to form a dopant band which overlaps with the conduction band of the material.

Similar to its parent indium oxide, ITO is generally nonstoichiometric with respect to oxygen, leading to the formula $\text{In}_{2-x}\text{Sn}_x\text{O}_{3-\delta}$. Delta (δ) depends on dopant concentration and synthesis conditions, but can be as high as 0.01 in undoped In_2O_3 (6). It is thought that in undoped and low-doped materials, the oxygen nonstoichiometry contributes to the conductivity of the material by donating two electron carriers per oxygen vacancy, forming shallow donor states approximately 0.03 eV below the conduction band (7, 8). Doping with Sn^{4+} can decrease the value of δ by the incorporation of compensating oxygen (9). For these reasons, samples of indium oxide and ITO are often reductively annealed to remove compensating oxygens and to maximize the number of oxygen vacancies in the material. In heavily doped materials, however, the contribution of oxygen vacancies to the conductivity is negligible compared to the carriers created by the dopant.

In the bulk, ITO is a solid solution with a tin concentration, $[\text{Sn}]$, of up to 6–10 cationic % dissolved in indium oxide, In_2O_3 (10, 11). Indium oxide crystallizes in the cubic bixbyite, or C-type rare earth, structure with $a = 10.117 \text{ \AA}$ (Table 1). The bixbyite structure can be derived from the fluorite structure by removing one-fourth of the anions. Indium oxide shares the bixbyite structure with the oxides of yttrium and scandium, as well as the smaller rare earth oxides, $Ln_2\text{O}_3$ ($Ln = \text{Tb-Lu}$). As a result, the oxides form complete solid solutions whose lattice parameters depend

¹ To whom correspondence should be addressed. E-mail: krp@nwu.edu. Fax: 847-491-7713

TABLE 1
Ionic Radii and Crystallographic Data of Selected Metal Oxides

Oxide	Lattice parameters (Å)	Metal ionic radius (Å) ^a	Structure type	Space group	Reference
In ₂ O ₃	<i>a</i> = 10.118	0.80	Bixbyite	<i>Ia</i> 3	PCPDF #06-0416 ^b
Y ₂ O ₃	<i>a</i> = 10.604	0.90	Bixbyite	<i>Ia</i> 3	PCPDF #43-1036 ^b
Sc ₂ O ₃	<i>a</i> = 9.485	0.75	Bixbyite	<i>Ia</i> 3	PCPDF #05-0629 ^b
SnO ₂	<i>a</i> = 4.7282 <i>c</i> = 3.1871	0.69	Rutile	<i>P4</i> 2/ <i>mmm</i>	PCPDF #41-1445 ^b
Y ₂ Sn ₂ O ₇	<i>a</i> = 10.373	—	Pyrochlore	<i>Fd</i> -3 <i>m</i>	PCPDF #20-1418 ^b
In ₄ Sn ₃ O ₁₂	<i>a</i> = 9.4604 <i>c</i> = 8.8584 ^c	—	Delta	<i>R</i> -3	(10)
Sc ₄ Sn ₃ O ₁₂	<i>a</i> = 9.353 <i>c</i> = 17.37 ^c	—	Delta	<i>R</i> -3	(18)

^a see Ref. (23).

^b PCPDFWIN Version 1.30, Joint Committee on Powder Diffraction Standards, International Center for Diffraction Data, 1997.

^c Hexagonal basis.

on the size and concentration of the lanthanide (12). In this paper, attempts to tin-dope the solid solutions In_{2-*x*}M_{*x*}O_{3-*δ*} (*M* = Y, Sc) will be reported, as well as the resulting structural, optical, and electrical properties of the products as they relate to ITO.

EXPERIMENTAL

Atomic percentages and concentrations are on a cation basis. Appropriate amounts of the pure oxides, In₂O₃, SnO₂, Y₂O₃, and Sc₂O₃ (Aldrich or Alpha Aesar, 99.99% cation purity), were weighed and thoroughly ground using an agate mortar and pestle, with acetone as a moistening agent. The acetone was evaporated, and the samples were uniaxially pressed under 7–8 MPa. The pellets were placed in covered alumina crucibles, heated for 2–4 days at 1250°C, reground and repelletized, and heated at 1400°C for 1–3 days. To prevent contamination from the alumina crucible and to minimize vaporization, the pellets were buried in a bed of sacrificial powder of the same composition as the sample. After the 1400°C heatings, the pellets were either air-quenched or quenched on a copper plate. Selected samples were reduced in tube furnaces under flowing 7% H₂/93% N₂ at temperatures ranging from 400–600°C. The as-fired tin-doped samples ranged in color from light to medium green, while their reduced counterparts ranged from a dark blue-green to blue-gray. Generally, the higher the tin concentration, the darker the pellet. The undoped (In_{1-*x*}M_{*x*})₂O_{3-*δ*} solid solutions ranged from white to light yellow with increasing indium.

X-ray powder diffraction patterns recorded on a Rigaku diffractometer (CuK α radiation, Ni filter, $2\theta = 10$ – 70° , 0.05 θ /step, 1 s/step counting time) and the Jade 5 XRD pattern processing program (13) were used to determine

reaction completion, phase composition, and lattice parameters. LiF (JCPDS No. 45-1460) was used as an internal standard.

Room temperature conductivity was measured with a linear, spring-loaded four-probe apparatus using a Keithly current source and voltmeter (models 225 and 197, respectively). Correction factors from Smits (14) were used to adjust for the geometry and finite thickness of the disc-shaped pellets. Because the electrical properties of TCOs depend heavily upon preparation methods, only samples which were prepared in this study were compared.

Conductivity and dc Hall measurements were taken from 4.2–340 K using a computer-controlled, five-probe technique (15). For the conductivity measurement, the voltage electrodes consisted of 25- μ m gold wire, placed approximately 0.5 cm apart. The voltage contacts on the samples were prepared with indium dots and the gold electrode wires were attached to these contacts with silver paste. On these materials, voltage contacts made with indium and silver paste were found to be superior to those made with only gold or silver paste. The current electrodes were 60- μ m gold wire and were attached to the ends of the samples with gold paste. Hall measurements utilized magnetic flux densities of 7400 Gauss and applied currents of 100 mA. All voltages were measured with a Keithley 181 nanovoltmeter.

Diffuse reflectance was used to determine the optical transmission of the as-fired and reduced pellets (16). A double-beam spectrophotometer (Cary 1E with Cary 1/3 attachment, Varian, USA) was used to measure diffuse reflectance of the bulk samples versus a polytetrafluoroethylene (PTFE) standard (Varian part number 04-101439-00), from 200–850 nm. The optical data were used to determine the maximum percent transmission (usually at 500 nm) and to estimate the optical band gap, which is roughly equal to the estimated onset of absorption of the material.

RESULTS AND DISCUSSION

 Y_2O_3 - In_2O_3 - SnO_2

Y_2O_3 is a white insulating powder with a unit cell larger than that of indium oxide (Table 1). As seen in Fig. 2, the lattice parameter increases linearly in the solid solution $(\text{In}_{1-x}\text{Y}_x)_2\text{O}_{3-\delta}$ as x increases, from 10.117 Å ($x = 0$) to 10.604 Å ($x = 1$). However, upon reaction of the solid solution with tin oxide, the yttrium oxide present in the system reacts with the tin oxide to form the pyrochlore $\text{Y}_2\text{Sn}_2\text{O}_7$. Similar to bixbyite, pyrochlore is an anion-deficient fluorite structure, and an insulator (17) with a band gap of 4.45 eV measured by diffuse reflectance. Tin oxide reacts with all the lanthanide oxides and Y_2O_3 to form the pyrochlore, $\text{A}_2\text{Sn}_2\text{O}_7$ (18). In our experiments X-ray powder diffraction shows formation of pyrochlore at tin or yttrium cation concentrations as low as 2%. This reaction diverts tin oxide from the solid solution, preventing it from donating charge carriers. $\text{Y}_2\text{Sn}_2\text{O}_7$ is a dominant thermodynamic phase at 1400°C, appearing throughout the ternary system, with the possible exception of indium-rich samples containing small concentrations of tin or yttrium oxide, in which case the small amount of pyrochlore could not easily be detected by powder diffraction.

The Y_2O_3 - In_2O_3 - SnO_2 ternary phase diagram can roughly be divided into three regions (Fig. 1). Two triangles consisting of $\text{SnO}_2/\text{In}_4\text{Sn}_3\text{O}_{12}/\text{Y}_2\text{Sn}_2\text{O}_7$ and $\text{Sn}/\text{In}_2\text{O}_3/\text{In}_4\text{Sn}_3\text{O}_{12}/\text{Y}_2\text{Sn}_2\text{O}_7$ exist on the right side of the diagram. Like bixbyite and pyrochlore, $\text{In}_4\text{Sn}_3\text{O}_{12}$ is an anion-deficient fluorite structure, forming at temperatures above 1250°C (16) (see Table 1). The remainder of the diagram consists of a two-phase region of essentially stoichiometric pyrochlore in equilibrium with a bixbyite solid solution. Figure 2 shows the Vegard's law behavior of the lattice parameters versus the percent yttrium oxide in

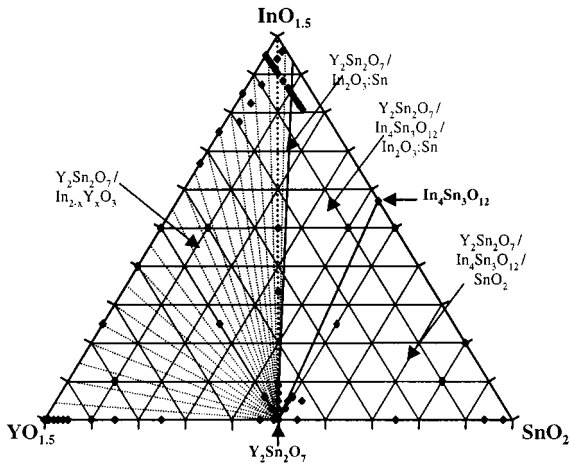


FIG. 1. The $\text{YO}_{1.5}$ - $\text{InO}_{1.5}$ - SnO_2 ternary phase diagram. The stoichiometries of the synthesized samples are shown (◆).

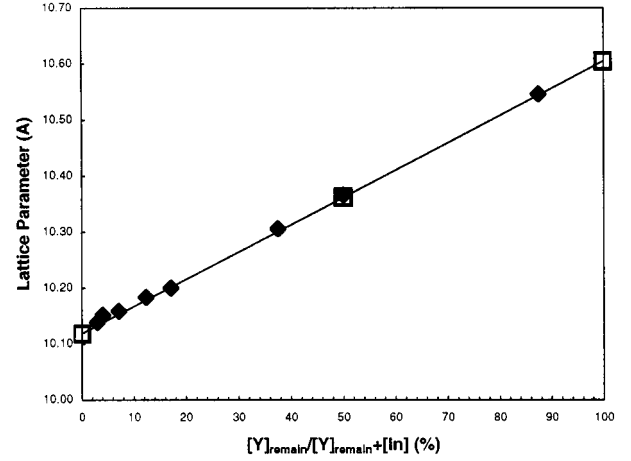


FIG. 2. Lattice parameters of the $(\text{In}_{1-x}\text{Y}_x)_2\text{O}_{3-\delta}$ solid solutions calculated from the solid solution/pyrochlore region (◆). The lattice parameters are compared to those calculated from the literature (□).

the bixbyite solid solution for the left half of the diagram, which is bounded by In_2O_3 , Y_2O_3 , and $\text{Y}_2\text{Sn}_2\text{O}_7$. The solid solution composition was calculated by assuming all the available tin oxide reacts with yttrium oxide to form $\text{Y}_2\text{Sn}_2\text{O}_7$. The remaining yttrium oxide then reacts with the indium oxide to form the solid solution:

$$[\text{Y}_2\text{O}_3]_{\text{total}} - [\text{Y}_2\text{O}_3]_{\text{pyrochlore}} = [\text{Y}_2\text{O}_3]_{\text{remain}}$$

$$\% \text{Y}_2\text{O}_3 = [\text{Y}_2\text{O}_3]_{\text{remain}} / ([\text{Y}_2\text{O}_3]_{\text{remain}} + [\text{In}_2\text{O}_3])$$

where $[\text{Y}_2\text{O}_3]_{\text{total}}$ represents the original percentage of yttrium oxide in the sample, $[\text{Y}_2\text{O}_3]_{\text{pyrochlore}}$ is the amount that reacts to form pyrochlore, and $[\text{Y}_2\text{O}_3]_{\text{remain}}$ is the percentage of yttrium oxide that remains to form the solid solution with indium oxide. The lattice parameter values correspond with the literature values calculated for the pure solid solution at the same yttrium oxide concentrations. The scavenging of tin by the pyrochlore phase apparently persists in the narrow extension of the two-phase (pyrochlore plus bixbyite) region to the right of the $\text{In}_2\text{O}_3/\text{Y}_2\text{Sn}_2\text{O}_7$ join. Here, stoichiometric pyrochlore is in equilibrium with what appears to be yttrium-free, Sn-doped In_2O_3 .

The electrical properties provide useful information concerning doping effects and also confirm the phase boundaries shown in Fig. 1 and the lattice parameter calculations in Fig. 2. A set of experiments was performed in the two-phase region, on a line of increasing yttrium concentration, with $[\text{Sn}] = 3\%$ (Fig. 3). The conductivity in Fig. 3 decreases rather dramatically (note the logarithmic scale) as Y^{3+} substitutes for In^{3+} in the bixbyite structure. At the same time, the optical band gap and percent transmission increase (Fig. 4). Although mobility can be significantly reduced by impurity scattering, such large changes are more

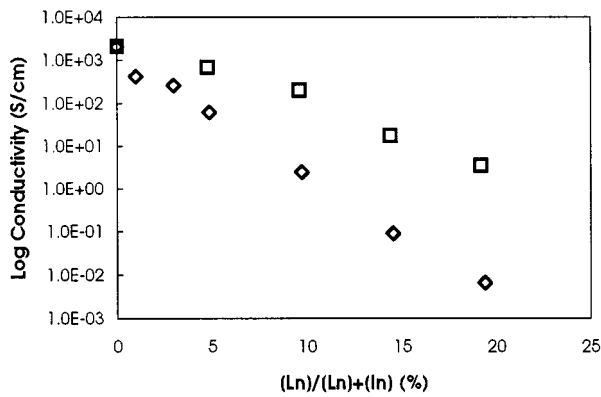


FIG. 3. Log conductivity vs [Y] (\diamond) and vs [Sc] (\square) in $(\text{In}_{0.97-x}\text{M}_x\text{Sn}_{0.03})_2\text{O}_{3-\delta}$ ([Sn] = 3%).

often associated with major reductions in carrier content, e.g., due to trapping of carriers. Yttrium oxide appears to be especially effective in this regard: 20% substitution of In^{3+} by Y^{3+} results in almost 6 orders of magnitude reduction in conductivity. In addition, substitution by yttrium oxide may limit the value of δ in $(\text{In}_{1-x-y}\text{Y}_x\text{Sn}_y)_2\text{O}_{3-\delta}$, i.e., minimize the oxygen vacancies, thereby decreasing the number of carriers.

A second set of experiments was conducted on a line of increasing [Sn] in a solid solution with a constant In:Y ratio of 95:5. The conductivity vs [Sn] data are shown in Fig. 5. There is an essentially monotonic increase in conductivity with composition from the low-conductivity $(\text{In}_{0.95}\text{Y}_{0.05})_2\text{O}_3$ solid solution through the $\text{In}_2\text{O}_3/\text{Y}_2\text{Sn}_2\text{O}_7$ join (at [Sn] = 5%) to the boundary of the $\text{In}_2\text{O}_3:\text{Sn}/\text{Y}_2\text{Sn}_2\text{O}_7/\text{In}_4\text{Sn}_3\text{O}_{12}$ tie-triangle (at [Sn] = 10%). Between 0 and 5% [Sn], the pyrochlore is in equilibrium with an increasingly In_2O_3 -pure bixbyite; i.e., the amount of yttrium in the solid solution decreases and the conductivity should increase, as observed in Fig. 5. Between 5 and 10% Sn, the pyrochlore is in equilibrium with an increasingly Sn-doped

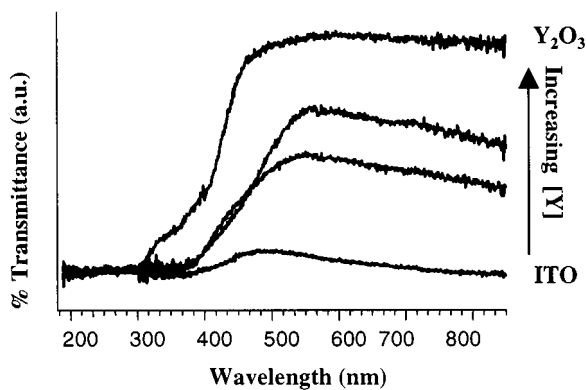


FIG. 4. Diffuse reflectance of $(\text{In}_{0.97-x}\text{Y}_x\text{Sn}_{0.03})_2\text{O}_{3-\delta}$ with varying [Y].

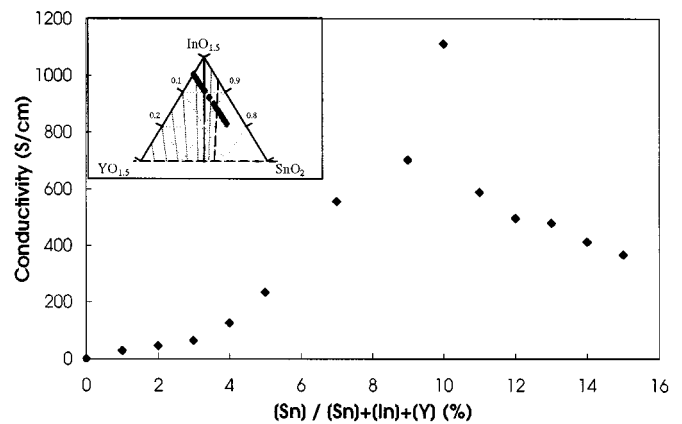


FIG. 5. Conductivity vs [Sn] in the solid solution $(\text{In}_{0.95-y}\text{Y}_{0.05}\text{Sn}_y)_2\text{O}_{3-\delta}$. Inset: Points on the phase diagram (from Fig. 1) corresponding to the stoichiometries of the samples in the graph.

In_2O_3 , and conductivity continues to rise. Upon crossing the phase boundary into the $\text{Sn}:\text{In}_2\text{O}_3/\text{Y}_2\text{Sn}_2\text{O}_7/\text{In}_4\text{Sn}_3\text{O}_{12}$ tie-triangle, conductivity exhibits a noticeable drop, but does not change as dramatically as [Sn] increases. The phase assemblage now consists of highly conductive Sn-doped In_2O_3 (major phase, but decreasing in amount) and two secondary phases— $\text{Y}_2\text{Sn}_2\text{O}_7$ (insulating) and $\text{In}_4\text{Sn}_3\text{O}_{12}$ (insulating and increasing in amount). The conductivity behavior of the samples described in Fig. 5, coupled with the lattice parameter calculations in Fig. 2, support the hypothesis that any available Y_2O_3 and SnO_2 in the system react to form $\text{Y}_2\text{Sn}_2\text{O}_7$, until one of the starting materials is completely scavenged.

$\text{Sc}_2\text{O}_3\text{-In}_2\text{O}_3\text{-SnO}_2$

Scandium oxide is a white insulating material with a unit cell smaller than that of In_2O_3 (Table 1). It forms a solid solution with In_2O_3 , $(\text{In}_{1-x}\text{Sc}_x)_2\text{O}_{3-\delta}$, and causes the unit cell of In_2O_3 to contract from 10.118 Å ($x = 0$) to 9.845 Å ($x = 1$). Unlike yttrium oxide, scandium oxide does not form the pyrochlore structure with tin oxide, although a second phase in the system, $\text{Sc}_4\text{Sn}_3\text{O}_{12}$, does exist (18, 19). This rhombohedral phase is isostructural with $\text{In}_4\text{Sn}_3\text{O}_{12}$, but it does not dominate the ternary system as does the pyrochlore in the Y–In–Sn oxide system. It is possible to substitute up to 6% tin oxide, which is approximately the tin solubility limit in pure In_2O_3 , into the $\text{In}_{2-x}\text{Sc}_x\text{O}_{3-\delta}$ solid solution ($x = 0.05, 0.10$) before detection of a second phase by powder diffraction. This makes it possible to study the effect of lattice contraction on the properties of ITO with single-phase samples. Tin oxide itself is not highly soluble in Sc_2O_3 , as attempts to synthesize the Sn-doped Sc_2O_3 analogue of ITO ([Sn] = 4%) resulted in a mixture of Sc_2O_3 and $\text{Sc}_4\text{Sn}_3\text{O}_{12}$.

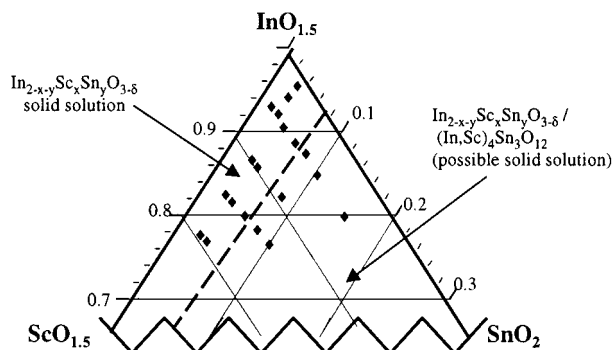


FIG. 6. Partial phase diagram of the $\text{ScO}_{1.5}\text{-InO}_{1.5}\text{-SnO}_2$ system.

Figure 6 shows the phase relations in the In-rich vortex of the Sc-In-Sn oxide ternary system. The complete ternary phase diagram has not yet been determined, although preliminary studies show the remainder of the diagram consists of mixtures of bixbyite, SnO_2 , $\text{Sc}_4\text{Sn}_3\text{O}_{12}$, and $\text{In}_4\text{Sn}_3\text{O}_{12}$. A complete or partial solid solution between the delta phases may also exist. Samples of $(\text{In}_{0.95}\text{Sc}_{0.05})_2\text{O}_{3-\delta}$ into which increasing amounts of tin oxide were substituted, while the In:Sc ratio was held constant at 95:5, were prepared, then reduced under forming gas. The reductions were performed in order to remove any compensating oxygen that might have been incorporated along with the tin dopant (6, 11). X-ray powder diffraction showed no change in the structure of the postannealed samples. Figure 7 shows the conductivities of both the reduced and unreduced 95:5 In:Sc solid solutions doped with tin, as well as reduced samples of ITO as a reference. All the reduced samples show increased conductivities compared to their unreduced counterparts. The conductivities of the reduced solid

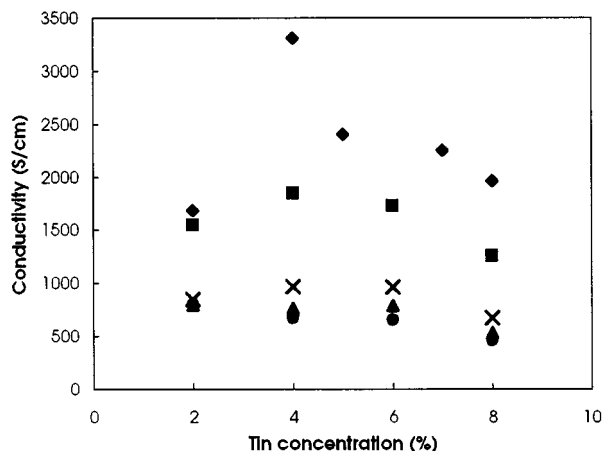


FIG. 7. Conductivity of reduced ITO (◆) and of $(\text{In}_{0.95}\text{-}_y\text{Sc}_{0.05})_2\text{O}_{3-\delta}$ doped with varying amounts of Sn, as-fired (●) and reduced in forming gas at 400°C (▲), 500°C (×), and 600°C (■).

solution samples are not as high as those of ITO, but are on the same order of magnitude.

The reduced materials show a shallow peak in conductivity at a tin concentration of about 4%. This is similar to that of prepared pure ITO samples both in this study and in the literature. Bates *et al.* (20) observed a large unexplained jump in conductivity at $[\text{Sn}] = 5\%$ in bulk ITO, while Frank and Köstlin (6) observed that in reduced ITO thin films an increasing amount of tin remained electrically inactive at concentrations above 4%. It is possible that under certain synthesis conditions, a tin concentration near 4% reflects the optimal carrier concentration with minimal scattering centers (e.g., Sn_2O_4 clusters)(11, 21). Alternatively, at concentrations above 4% small amounts of $\text{In}_4\text{Sn}_3\text{O}_{12}$ delta phase may be forming. Because the major peaks of the delta phase overlap with those of the bixbyite solid solution, it is possible that small quantities of the delta phase crystallize undetected by X-ray diffraction. In Sc:In solid solution oxide samples with a tin concentration of approximately 6–8%, we begin to see $\text{In}_4\text{Sn}_3\text{O}_{12}$ appear on powder patterns; at lower concentrations, the results are ambiguous (Fig. 8).

The addition of Sc_2O_3 to the ITO system causes a decrease in conductivity and an increase in transparency, as well as a steady decrease in the lattice parameter. Figure 3 shows the decrease in conductivity for unreduced samples containing 3% tin with varying ratios of indium and scandium. For analogous In:Sc solid solution samples in which $[\text{Sn}] = 4\%$, the same trend is observed. At lower scandium concentrations, the samples containing 4% tin show higher conductivities than their $[\text{Sn}] = 3\%$ analogues, although

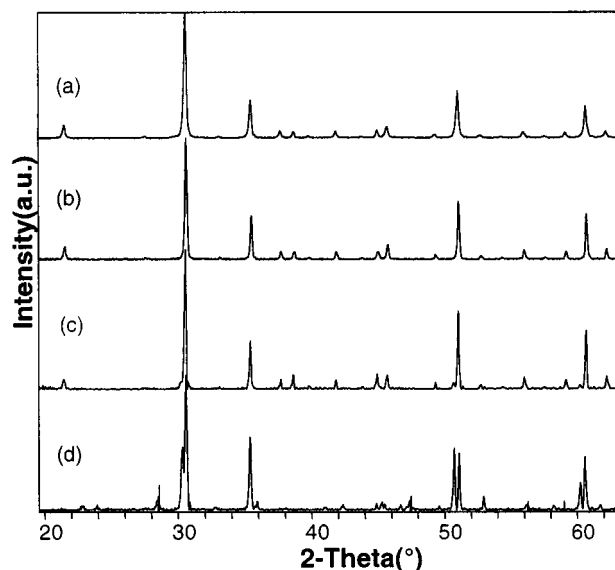


FIG. 8. Powder X-ray diffraction patterns of (a) In_2O_3 , (b) $(\text{In}_{0.95}\text{Sc}_{0.05})_2\text{O}_{3-\delta}$ solid solution doped with 4% Sn, (c) $(\text{In}_{0.95}\text{Sc}_{0.05})_2\text{O}_{3-\delta}$ solid solution doped with 10% Sn, and (d) $\text{In}_4\text{Sn}_3\text{O}_{12}$.

they even out at higher scandium concentrations. Reductively annealed samples exhibit conductivities up to an order of magnitude larger than their as-fired counterparts. These trends are similar to those of the Y_2O_3 - In_2O_3 - SnO_2 system, yet the conductivities of the Sc samples are on the order of 10^2 - 10^3 S/cm higher, depending on their composition (Fig. 3). This is most likely due to the absence of an Sn-scavenging pyrochlore phase, as opposed to the Y-In-Sn oxide system, and the resulting ability to Sn-dope the bixbyite phase, even with substantial Sc^{3+} substitution for In^{3+} . The decrease in conductivity in the Sc system compared to that of ITO may have several causes, including lower mobility, lower carrier concentrations, or the insulating properties of Sc_2O_3 . Diffuse reflectance (Fig. 9) shows that in these samples, the optical band gaps of the 95:5 and 90:10 samples are lower than that of ITO. The lower optical band gaps relative to ITO imply either fewer carriers in the scandium system, owing to the Moss-Burstein shift (22), or a narrowing of the band gap. The larger band gap of the 80:20 sample is influenced by the increased presence of insulating Sc_2O_3 , which has a much larger band gap than that of ITO. Also, since this sample is not degenerate, no Moss-Burstein shift would be apparent.

Hall measurements were performed on as-fired samples containing 4% Sn and varying In:Sc ratios of 1:0 (ITO), 95:5, and 80:20. All materials were observed to be *n*-type conductors. The ITO and 95:5 samples exhibit metallic behavior, with a slight decrease in conductivity with increasing temperature (Fig. 10) and carrier concentrations on the order of 10^{20} cm^{-3} , illustrative of degenerate semiconductors which display metallic conductivity. The 80:20 sample, on the other hand, appears semiconducting as its conductivity increases with temperature. The carrier concentration of this sample drops an order of magnitude to approximately 2×10^{19} cm^{-3} , consistent with its semiconductive character. This decrease in carrier concentration may be due to either

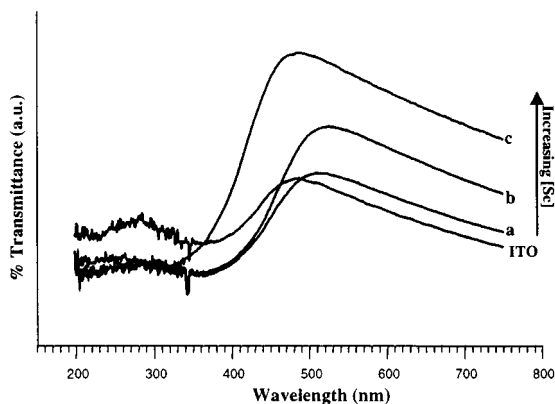


FIG. 9. Diffuse reflectance of ITO (4% Sn) and $(In_{0.96-x}Sc_xSn_{0.04})_2O_{3-\delta}$ with an In:Sc ratio of (a) 95:5, (b) 90:10, and (c) 80:20.

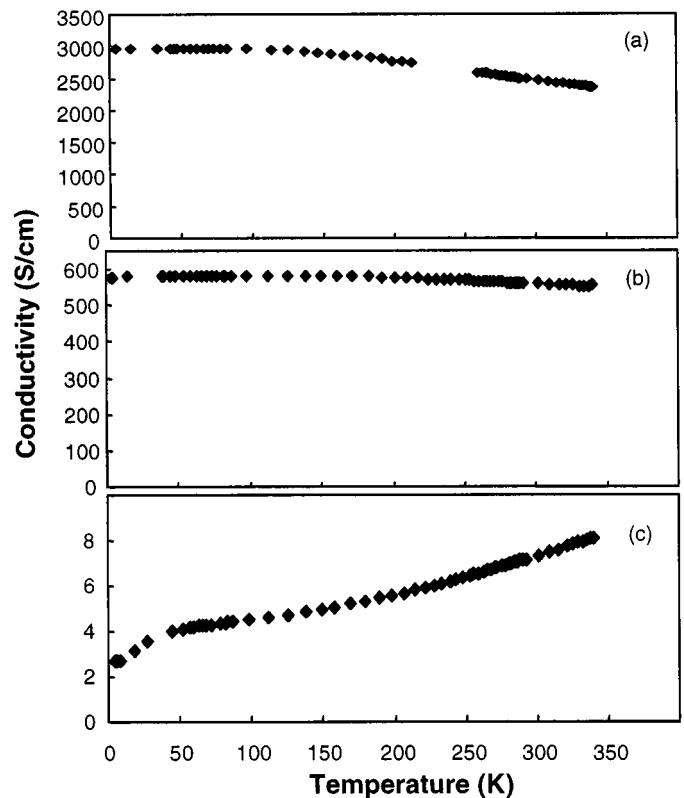


FIG. 10. Conductivity vs temperature for (a) ITO ([Sn] = 4%), (b) $(In_{0.95}Sc_{0.05})_2O_{3-\delta}$ solid solution doped with 4% Sn, and (c) $(In_{0.8}Sc_{0.2})_2O_{3-\delta}$ solid solution doped with 4% Sn.

the formation of neutral complexes (see below) and/or a reduction in oxygen vacancies upon incorporation of scandium.

The mobilities of the samples decrease dramatically as scandium is added, from approximately 48 $cm^2/V \cdot s$ for ITO to about 16 $cm^2/V \cdot s$ and 2 $cm^2/V \cdot s$ for the 95:5 and 80:20 samples, respectively. Mobility can be affected by such things as grain boundaries and scattering centers. In ITO, scattering centers such as Sn_2O_i (i = interstitial) and Sn_2O_4 are known to form. Frank and Köstlin (6) state that Sn_2O_i forms when two Sn^{4+} cations coordinate with an interstitial oxygen. Sn_2O_i often dissociates under reducing conditions, allowing each tin to donate an electron carrier. Judging by the large increase in conductivity between reduced $(In_{1-x-y}Sc_xSn_y)_2O_{3-\delta}$ samples and their unreduced counterparts, the existence of this complex is a distinct possibility. Sn_2O_4 is formed when two Sn^{4+} cations on nearest-neighbor sites bond with three nearest-neighbor oxygens and one O^{2-} located on a nearest-neighbor vacancy in the fluorite-deficient bixbyite structure. It cannot be dissociated by reduction and permanently removes two tins from the dopant pool (6). As the volume of the $(In_{1-x-y}Sc_xSn_y)_2O_{3-\delta}$ unit cell decreases, and the substituting Sn^{4+} ions become more concentrated, it is possible that

the formation of this neutral complex is facilitated. The formation of Sn_2O_4 could account for the dramatic decrease in mobility as scandium is added to the system, as well as the decline in carrier concentration in the 80:20 sample as fewer tin atoms donate electron carriers. Another cause for the decrease of carriers may be the formation of $\text{In}_4\text{Sn}_3\text{O}_{12}$, which would remove tin carriers and could act as scattering centers, adversely affecting the mobility as well. Pattern matching and refinements of samples are inconclusive with respect to detecting the second phase, as many of the peaks overlap with those of the dominant bixbyite structure.

CONCLUSIONS

Solid solutions of the type $(\text{In}_{1-x}\text{M}_x)_2\text{O}_{3-\delta}$ ($M = \text{Y}, \text{Sc}$) have been doped with tin and their electrical, optical, and structural properties investigated. When $M = \text{Y}$, the tin oxide reacts with yttrium oxide to form the pyrochlore $\text{Y}_2\text{Sn}_2\text{O}_{12}$, which dominates the ternary phase system. Increasing the concentration of tin oxide causes a decrease in conductivity and an increase in percent transmission and band gap, most likely caused by the presence of the insulating pyrochlore phase. The lattice parameters of the solid solution decrease with increasing scandium concentration when $M = \text{Sc}$, and up to 6–8% tin oxide can be added before the delta phase is detected by powder X-ray diffraction. As in the yttrium system, increasing the scandium concentration causes a decrease in conductivity and an increase in transmission. Hall measurements of doped $(\text{In}_{2-x}\text{Sc}_x)\text{O}_{3-\delta}$ ($x = 0.1, 0.4$) solid solutions show a sharp drop in mobility and a decrease of the carrier concentration as scandium is added. The large reduction in mobility may be caused by an increase in scattering centers as the unit cell volume decreases, and possibly the presence of a second phase, $\text{In}_4\text{Sn}_3\text{O}_{12}$ or an $(\text{In},\text{Sc})_4\text{Sn}_3\text{O}_{12}$ solid solution.

ACKNOWLEDGMENTS

This work was supported by the MRSEC program of the National Science Foundation (DMR-9632472) at the Materials Research Center of Northwestern University. A.D. was supported by the Materials Research Center Undergraduate Summer Research program.

REFERENCES

1. K. L. Chopra, S. Major, and D. K. Pandya, *Thin Solid Films* **102**, 1 (1983).
2. I. Hamberg and C. G. Granqvist, *J. Appl. Phys.* **60**, R123 (1986).
3. Z. M. Jarzebski, *Phys. Stat. Sol. (a)* **71**, 13 (1982).
4. J. C. Manificier, *Thin Solid Films* **90**, 297 (1982).
5. N. R. Lynam, *Proceedings of the Symposium on Electrochromic Materials—Electrochem. Soc. Proc.* **90–92**, 201 (1990).
6. G. Frank and H. Köstlin, *Appl. Phys. A* **27**, 197 (1982).
7. J. C. C. Fan and J. B. Goodenough, *J. Appl. Phys.* **48**, 3524 (1977).
8. R. L. Weiher, *J. Appl. Phys.* **33**, 2834 (1962).
9. T. Omata, H. Fujiwara, S. Otsuka-Yao-Matsuo, N. Ono, and H. Ikawa, *Jpn. J. Appl. Phys.* **2** **37**, L879 (1998).
10. N. Nadaud, N. Lequeux, M. Nanot, J. Jove, and T. Roisnel, *J. Solid State Chem.* **135**, 140 (1998).
11. G. Frank, H. Köstlin, and A. Rabenau, *Phys. Stat. Sol. A* **52**, 231 (1979).
12. R. S. Roth and S. J. Schneider, *J. Res. Nat. Bur. Stand. A* **64**, 317 (1960).
13. "JADE", Version 5.0.16, Materials Data Inc., Livermore, CA, 1999.
14. F. M. Smits, *Bell Syst. Tech. J.* **37**, 711 (1958).
15. J. W. Lyding, H. O. Marcy, T. J. Marks, and C. R. Kannewurf, *IEEE Trans. Instrum. Meas.* **37**, 76 (1988).
16. H. Hecht in "Modern Aspects of Reflectance Spectroscopy" (W. Wendlandt, Ed.), Plenum, New York, 1968.
17. M. A. Subramanian, G. Aravamudan, and G. V. Subba Rao, *Prog. Solid State Chem.* **15**, 55 (1983).
18. F. Brisse and O. Knop, *Can. J. Chem.* **46**, 859 (1968).
19. M. B. Varfolomeev, A. S. Mironova, and N. T. K. Nien, *Russ. J. Inorg. Chem.* **20**, 2038 (1975).
20. J. L. Bates, C. W. Griffin, D. Marchant, and J. E. Garnier, *Am. Ceram. Soc. Bull.* **65**, 673 (1986).
21. R. B. H. Tahar, T. Ban, Y. Ohya, and Y. Takahashi, *J. Appl. Phys.* **83**, 2631 (1998).
22. E. Burstein, *Phys. Rev.* **93**, 632 (1954).
23. R. D. Shannon, *Acta Crystallogr. A* **32**, 751 (1976).